Biophysical Journal Volume 73 August 1997 1110–1117

High-Gain, Low-Noise Amplification in Olfactory Transduction

Steven J. Kleene
Department of Cell Biology, Neurobiology and Anatomy, University of Cincinnati, Cincinnati, Ohio 45267-0521 USA

ABSTRACT It is desirable that sensory systems use high-gain, low-noise amplification to convert weak stimuli into detectable signals. Here it is shown that a pair of receptor currents underlying vertebrate olfactory transduction constitutes such a scheme. The primary receptor current is an influx of Na^+ and Ca^{2+} through cAMP-gated channels in the olfactory cilia. External divalent cations improve the signal-to-noise properties of this current, reducing the mean current and the current variance. As Ca^{2+} enters the cilium, it gates Cl^- channels, activating a secondary depolarizing receptor current. This current amplifies the primary current, but introduces little additional noise. The system of two currents plus divalent cations in the mucus produces a large receptor current with very low noise.

INTRODUCTION

To detect weak stimuli, sensory neurons often amplify the initial signal one or more times. The amplified signal then becomes sufficient to trigger an action potential and/or the release of neurotransmitter. Depending on the mechanism of amplification, it may also be possible to selectively amplify the signal relative to chemical or electrical fluctuations that occur in the absence of stimulus (noise). All of this can increase the reliability and sensitivity of stimulus detection.

Amplification is used by the sensory system that detects odorants. In vertebrates, detection and transduction of odorous stimuli occur in the cilia of olfactory receptor neurons (Kurahashi, 1989; Firestein et al., 1990; Lowe and Gold, 1991). Initially, odorant molecules may interact with specific transmembrane receptors on the olfactory cilia (Buck and Axel, 1991). A bound receptor protein may then interact with a GTP-binding protein (G-protein), which can activate a ciliary adenylate cyclase (Pace et al., 1985; Shirley et al., 1986; Sklar et al., 1986; Lowe et al., 1989; Bruch and Teeter, 1990; Boekhoff et al., 1990). The cAMP formed directly gates ciliary channels (Nakamura and Gold, 1987), resulting in a primary depolarizing receptor current carried by Na^+ and Ca^{2+}. When sufficient Ca^{2+} accumulates in the cilium, it can gate ciliary Cl^- channels. The result is a secondary receptor current, also depolarizing, but carried by Cl^- (Kurahashi and Yau, 1993; Kleene, 1993b; Lowe and Gold, 1993; Firestein and Shepherd, 1995; Zhainazarov and Ache, 1995).

Although the complete stoichiometry has not been demonstrated, it is likely that amplification occurs three times during this scheme. First, a bound receptor protein may activate several G-protein molecules, each of which could activate one cyclase molecule. An activated cyclase will in turn produce many molecules of cAMP, each of which could contribute to the gating of a cationic channel. Finally, each cAMP-gated channel will allow entry of many Ca^{2+} ions, each of which could help to gate a Cl^- channel. Each amplifying step has the potential to increase the signal relative to background noise. It is also possible, however, that the mechanism of amplification itself could introduce substantial fluctuation. At each stage, the ideal amplifier would have a high gain but introduce little additional noise (Block, 1992).

The signal-to-noise properties of the olfactory signal amplifiers have not previously been investigated. It is clear that background current noise can be substantial (Lowe and Gold, 1995) and that the primary cationic current can be greatly amplified by the secondary Cl^- current (Kleene, 1993b; Lowe and Gold, 1993). Here it is shown that this high-gain amplification occurs with very little increase in noise.

MATERIALS AND METHODS

Ciliary patch procedure

Northern grass frogs (*Rana pipiens*) were decapitated and pithed. Single receptor neurons were isolated from the olfactory epithelium as described elsewhere (Kleene and Gesteland, 1991a). Cell suspensions were prepared in a standard extracellular solution (shown in Table 1 as the solution used to study the biphasic currents). A single receptor neuron was placed in an extracellular bath containing this solution. One cilium of a neuron was sucked into a patch pipette until a high-resistance seal formed near the base of the cilium. The pipette contained one of the extracellular solutions shown in Table 1. Small amounts of bath solution entered the pipette tip during the patch procedure. However, within 1 min the current-voltage relation reached a stable state that depended on the bulk pipette solution (Kleene, 1993a). The pipette was raised briefly into the air, causing excision of the cilium from the cell. The cilium remained sealed inside the recording micropipette with the cytoplasmic face of the membrane exposed to the bath. The pipette containing the cilium could be quickly transferred through the air to various pseudointracellular baths without rupturing the seal. Additional details of the ciliary patch procedure have been presented elsewhere (Kleene and Gesteland, 1991a; Kleene, 1995b).

Received for publication 13 February 1997 and in final form 24 April 1997.

Address reprint requests to Dr. Steven J. Kleene, Department of Cell Biology, Neurobiology and Anatomy, P.O. Box 670521, University of Cincinnati, Cincinnati, OH 45267-0521. Tel.: 513-558-6099; Fax: 513-558-4454; E-mail: steve@syrano.acb.uc.edu.

0006-3495/97/08/1110/08 $2.00

TABLE 1 Compositions of solutions (mM)

	NaCl	KCl	$CaCl_2$	$MgCl_2$	EDTA	NaOH
Extracellular						
cAMP study, unblocked	100	16.9	—	—	1	4
cAMP study, blocked	100	16.9	1	2	—	1
Ca^{2+} study	117	1.14	1	2	—	1
Biphasic currents	115	3	1	2	—	1

	NaCl	KCl	$MeSO_3H$	cAMP	$CaCl_2$	$MgCl_2$	BAPTA	Dibromo-BAPTA	NaOH	KOH
Pseudointracellular										
cAMP studies	5	10.7	99.3	0.004–0.3	1	—	2	—	—	108
Ca^{2+} study	115	—	—	—	0.12–2.29	2	—	2	1	—
Biphasic currents	5	110	—	—	1.2	—	3	—	—	13

Abbreviations used: $MeSO_3H$, methanesulfonic acid; BAPTA, 1,2-bis(2-aminophenoxy)ethane-*N,N,N′,N′*-tetraacetic acid; dibromo-BAPTA, 1,2-bis(2-amino-5-bromophenoxy)ethane-*N,N,N′,N′*-tetraacetic acid, tetrapotassium salt. All solutions contained 5 mM HEPES and were adjusted to pH 7.2. The NaOH and KOH listed include amounts necessary to titrate EDTA, BAPTA, and $MeSO_3H$, which are listed as free acids. $[Ca^{2+}]_{free}$ in the pseudointracellular solutions was 0.15 μM in both cAMP studies, 0.1–300 μM in the Ca^{2+} study, and 0.1 μM in the studies of biphasic currents. In experiments that used reduced Ca^{2+} buffering, BAPTA was reduced to 0.5 mM.

Solutions

The solutions used are listed in Table 1. To study noise from the individual channel types, it was advantageous to minimize current through a resting ciliary K^+ conductance (Kleene, 1992). This was done by setting the equilibrium potential for K^+ at −50 mV, which was at or near the holding potential. To study noise from the cAMP-gated channels, it was also necessary to minimize current through the Ca^{2+}-activated Cl^- channels. To do this, the equilibrium potential for Cl^- was set at −50 mV by replacing most internal Cl^- with methanesulfonate$^-$. Niflumic acid was avoided as a Cl^--channel blocker, because it also increases the noise of the cAMP-activated current (Kleene and Gesteland, 1991b). Standard solutions were used to study the biphasic currents (Table 1).

Previously reported constants and methods (Kleene and Gesteland, 1991b; Kleene and Cejtin, 1994) were used to calculate $[Ca^{2+}]_{free}$. Noise properties of the Ca^{2+}-activated Cl^- current were studied in solutions like those previously described (Kleene and Gesteland, 1991b). The half-maximum current is seen when cytoplasmic $[Ca^{2+}]_{free}$ is near 5 μM. Dibromo-BAPTA was used to effectively buffer $[Ca^{2+}]_{free}$ in this range. In all other experiments, BAPTA was used to buffer $[Ca^{2+}]_{free}$ at 0.1–0.15 μM.

Electrical recording

Both the recording pipette and chamber were coupled to a List L/M-EPC7 patch-clamp amplifier by Ag/AgCl electrodes. The 50-GΩ headstage resistor was used, except with the largest currents. All recordings were made under voltage clamp at room temperature (25°C). The current was adjusted to zero with the open pipette in the well in which the patching procedure was carried out. Corrections were made for liquid junction potentials at the pipette tip; these were 6 mV at most. The recording chamber has been described in detail elsewhere (Kleene, 1995b). The amplifier signal was filtered at 3 kHz with an 8-pole low-pass Bessel filter (model 902L; Frequency Devices, Haverhill, MA). Frequency cutoffs of other elements in the system were all above 3 kHz. Current was sampled at 7 kHz by the Axotape program (Axon Instruments, Foster City, CA). Except when the power density spectra were generated (Fig. 4), records were subjected to a second low-pass filtering at 100 Hz, by using the Digital Filter program (a gift of Horst Fischer, University of California at Berkeley). Potentials are reported as bath (cytoplasmic) potential relative to pipette potential.

Voltage jumps were generated by pCLAMP software (Axon Instruments). Membrane potential was maintained at 0 mV between jumps. To study current noise from the cAMP-gated channels, current was recorded for 20 s at −50 mV in a control bath containing no cAMP. This process was repeated as the cilium was moved through baths containing increasing concentrations of cAMP. The study of noise from the Ca^{2+}-gated channels was conducted in the same way, except that membrane potential was held at −40 mV for 10 s. The smaller potential and duration were necessary because the seals were less stable in the Ca^{2+}-containing baths. To facilitate comparisons of the two currents, results of the Ca^{2+}-activated Cl^- study in Fig. 2 and Table 2 have been extrapolated from −40 mV to −50 mV. To do this, the Cl^- current amplitudes were multiplied by 1.25 (50 mV/40 mV). Variances of the Cl^- current were multiplied by 1.25^2 (see

TABLE 2 Comparison of cAMP- and Ca^{2+}-activated ciliary currents

	cAMP-activated cationic (n = 5–7)	Ca^{2+}-activated Cl^- (n = 6)	Difference
Mean saturating current (pA)	−41 ± 8	−50 ± 6	NS
Variance of saturating current (pA^2)	0.43 ± 0.10	0.16 ± 0.03	$p < 0.05$
Single-channel current (i, fA)	−28 ± 1	−25 ± 3	NS
Single-channel conductance (g, pS)	0.56 ± 0.02	0.50 ± 0.06	NS
Maximum open probability (p_{max})	0.68 ± 0.03	0.97 ± 0.06	$p < 0.001$
Channels per cilium (n)	2470 ± 820	2650 ± 680	NS

For each cilium, mean current and current variance were measured in a series of cytoplasmic baths containing increasing concentrations of cAMP or Ca^{2+} (see Materials and Methods). Values assume a holding potential of −50 mV (see Materials and Methods). The final concentrations were saturating doses. The last four values shown were estimated by linear regression as described for Fig. 2 *B*. The average correlation coefficient r was 0.94; two data sets with $r < 0.8$ were eliminated when the single-channel parameters were estimated. With currents of these amplitudes, errors due to the ciliary cable properties are small (Larsson et al., 1997). NS, No significant difference ($p > 0.3$).

Eq. 3). The Cl^- current-voltage relation was linear in this voltage range and reversed near 0 mV.

During the study of biphasic currents, the duration of the first phase increased as the holding potential was made less negative (Kleene and Gesteland, 1991b). A holding potential was chosen such that the mean current during the first phase was stable for at least 0.5 s. No controls have been recorded from the biphasic current results shown.

Results of repeated experiments are reported as mean ± SEM. Student's *t*-test was used for statistical comparisons. Significance levels are reported for two tails.

Calculation of variance

In some cases, noise records showed slow baseline drift. Using a mean derived from the whole record would have resulted in large variance contributions from each end of the record. For this reason, the variance contribution of each point was figured against a local mean, which was the average of the 3500 points (0.5 s) surrounding the given point. This eliminated the slow drift and any variance from noise at frequencies that were <2 Hz. With the exception of the power density spectra (Fig. 4), all numerical values were figured from records after correction for slow changes in mean current. The current recordings in Figs. 1 and 3 are shown before the correction.

Power spectral analysis of biphasic currents

Power density spectra were calculated from current records such as those shown in Fig. 3. For the control spectrum, a 12-s portion of the record in the absence of cAMP (Fig. 3 *A*) was split into 20 segments of 4096 points (585 ms) each. A power density spectrum was generated from each of the 20 segments. Each spectrum consisted of a power density value for each of 4096 frequencies. For each frequency, the 20 power density values from the individual spectra were averaged, and this average spectrum is shown in Fig. 4. Current records used for the other two spectra were taken from Fig. 3 *B* and three other repeats of that experiment on the same cilium. From those four records, a total of 20 4096-point segments were obtained for each of the two steady-state phases in the presence of cAMP, and these were analyzed in the same way as the control. Pairs of points were compared statistically by using the 20 values for each point before averaging. No controls were subtracted from any of the current records or spectra.

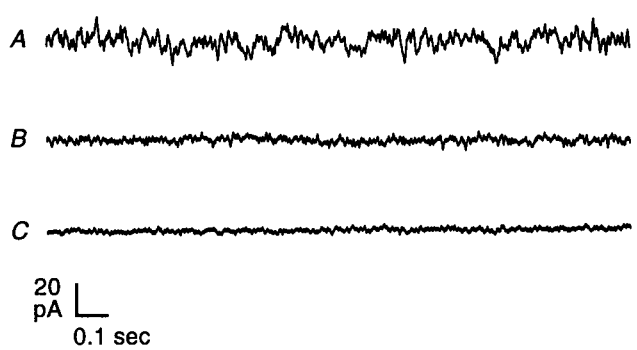

FIGURE 1 Currents activated by cytoplasmic cAMP or Ca^{2+} in olfactory cilia. Steady-state currents were measured under voltage clamp in three olfactory cilia. (*A*) Current activated by 1.5 μM cAMP in the absence of external Ca^{2+} and Mg^{2+}, $V = -50$ mV. (*B*) Current activated by 38 μM cAMP with external Mg^{2+} (2 mM) and Ca^{2+} (1 mM), $V = -50$ mV. (*C*) Current activated by 4.8 μM Ca^{2+}, $V = -40$ mV. Mean currents were −37 pA (*A*), −36 pA (*B*), and −35 pA (*C*). Current variances were 5.15 pA^2 (*A*), 0.64 pA^2 (*B*), and 0.23 pA^2 (*C*). These values were calculated from the full records, which were 20 s (*A* and *B*) or 10 s (*C*). Currents measured in the absence of cAMP and Ca^{2+} have not been subtracted from the records shown, but were subtracted before the means and variances were calculated.

RESULTS

Electrical recordings were made from single frog olfactory cilia. Each cilium was sealed inside a patch pipette and excised from the cell, so that the cytoplasmic face of its membrane was exposed to the bath (Kleene and Gesteland, 1991a). The currents responsible for olfactory transduction could then be activated by adding cAMP or Ca^{2+} to the bath.

Signal-to-noise properties of the components of the olfactory receptor current

Steady-state currents activated by cAMP or Ca^{2+} were measured near the neuronal resting potential. Fig. 1 shows three such current records. Although the mean currents of these records were nearly equal, the current variances differed greatly. This preliminary result suggested that the variance might depend strongly on the type of channel gated and, for the cAMP-activated current, the level of external divalent cations. It was not possible to simultaneously match the number of channels or the channel open probabilities, on which the variances should also depend.

The mean current and the variance of the current were measured for many such records representing the full dose-response ranges for cAMP and Ca^{2+} (Fig. 2 *A*). When not blocked by external divalent cations, the cAMP-gated channels produced the largest currents and variances (Fig. 2 *A*, *open circles*). These currents averaged −108 ± 14 pA, and their average variance was 5.1 ± 0.6 pA^2 ($n = 35$). The addition of external Ca^{2+} and Mg^{2+} significantly reduced both the mean current and current variance of the cAMP-activated currents ($p < 0.001$, Fig. 2 *A*, *filled circles*). The average current in this case was −24 ± 3 pA, and the variance averaged 0.35 ± 0.04 pA^2 ($n = 34$). The Ca^{2+}-activated Cl^- currents had amplitudes and variances that averaged −27 ± 2 pA and 0.21 ± 0.02 pA^2, respectively (Fig. 2 *A*, *open triangles*, $n = 54$). The pooled variances from the Cl^- channels were significantly lower than those from the cAMP-gated channels blocked by divalent cations ($p < 0.001$). There was no significant difference between the corresponding pooled mean currents ($p > 0.4$).

Plots of current variance versus mean current for individual cilia are shown in Fig. 2, *B* and *C*. In theory (DeFelice, 1981), such plots should be parabolas of the form

$$\sigma^2 = iI - I^2/n \quad (1)$$

where σ^2 is the current variance, i is the current through a single channel, I is the mean macroscopic current amplitude, and n is the number of channels in the cilium. The initial slope of the plot (at $I = 0$) equals i. Typically, the cAMP-gated currents blocked by divalent cations (Fig. 2 *B*) showed somewhat larger variances than the Ca^{2+}-activated

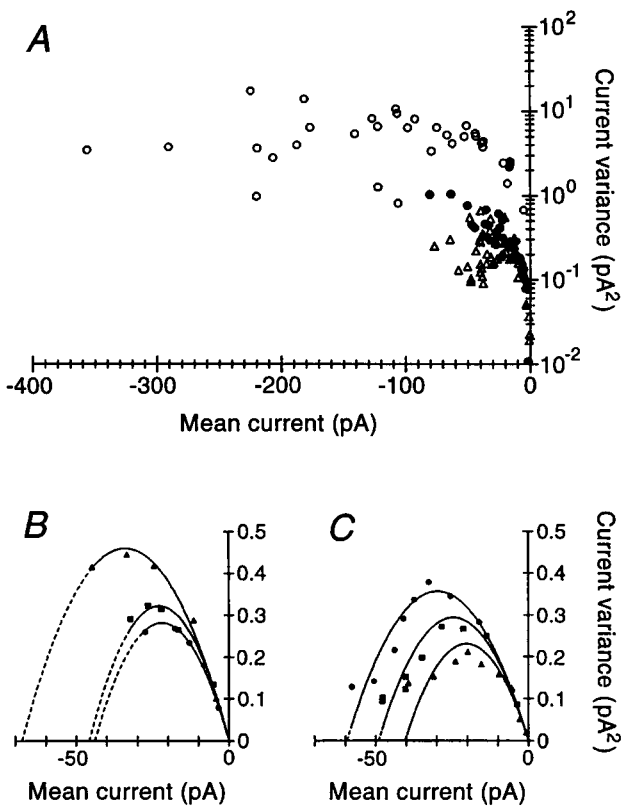

FIGURE 2 Signal-to-noise properties of the cAMP- and Ca^{2+}-activated ciliary currents. The mean current and current variance of steady-state ciliary currents activated by cytoplasmic second messengers were measured as described in Materials and Methods. (*A*) Current and current variance measurements pooled from all determinations. The variance is plotted on a logarithmic scale to allow better discrimination of the points. Current was activated by cAMP in the absence of external Ca^{2+} and Mg^{2+} (○; $V = -50$ mV; 0.4–300 μM cAMP; results from seven cilia); cAMP in the presence of external Ca^{2+} and Mg^{2+} (●; $V = -50$ mV; 4–300 μM cAMP; results from seven cilia); and Ca^{2+} (△; 1–300 μM free Ca^{2+}; $V = -40$ mV; results from six cilia). Mean current and current variance in the control bath were subtracted from the corresponding values measured in the presence of second messengers. The control values averaged -8 ± 1 pA and 0.03 ± 0.01 pA², respectively ($n = 20$). Saturating currents were measured with 300 μM of the second messenger. (*B*) Current variance versus mean current for each of three cilia exposed to 4–300 μM cAMP in the presence of external Ca^{2+} and Mg^{2+} at −50 mV. Data from each cilium were fit by linear least-squares regression to a plot of σ^2/I versus I according to the following transformation of Eq. 1: $\sigma^2/I = i - I/n$ (Kurahashi and Kaneko, 1993). This gave estimates of i (the y intercept) and n (−1/slope). The curves shown resulted from using these estimated values in Eq. 3 (Discussion) and plotting as p increased from 0 to 1. Where predicted current exceeded that measured with a saturating dose of ligand, the curved is shown as dashed. (*C*) Variance versus mean current for each of three cilia exposed to 1–300 μM free Ca^{2+} at −40 mV. Values shown have been extrapolated to −50 mV as described in Materials and Methods. Analysis is as described for Fig. 2 *B*.

Cl^- currents (Fig. 2 *C*). The plots also indicate that the divalent-blocked cAMP-gated channel has a much lower maximum open probability (p_{max}) than the Cl^- channel. For each parabola, p_{max} is estimated by dividing the largest mean current observed by the left-hand x intercept of the parabola (where the open probability p is 1.0). For each cilium, the largest current shown was measured with a saturating dose of ligand (cAMP or Ca^{2+}). The results of several such experiments are summarized in Table 2. For the two currents, no significant differences were observed between the saturating current amplitudes (Kleene, 1993b), the numbers of channels per cilium (Larsson et al., 1997), or the single-channel conductances. (Note that the cationic unit conductance and mean current are much larger when external Ca^{2+} and Mg^{2+} are absent (Frings et al., 1992; Kleene et al., 1994; Larsson et al., 1997.)) A striking difference is that p_{max} can reach nearly 1.0 for the Ca^{2+}-activated Cl^- channels, but averages just 0.68 for the cAMP-gated cationic channels. As a result, current through the divalent-blocked cAMP-gated channels had a significantly greater variance at saturation than the Ca^{2+}-activated Cl^- current (see Discussion).

When single-channel parameters are inferred from noise analysis, their values depend on the range of frequencies analyzed. With low-pass filtering at 3 kHz (Larsson et al., 1997), the Cl^- channel was estimated to have a larger unit conductance (0.8 pS) and a smaller p_{max} (0.61). In this report, frequencies above 100 Hz were excluded in an attempt to mimic low-pass filtering by the resistance and capacitance of the intact neuron. This reduces total variance without changing the mean current. Lower filtering thus reduces the inferred unitary current i, which is the variance/mean ratio as $p \rightarrow 0$ (see Fig. 2 *B*). This value of i is the unitary current that will be seen after low-pass filtering by the neuron. Low-pass filtering increases the apparent p_{max} but does not affect the estimated number of channels n. For comparison with previous results, the current records used for Table 2 were also analyzed with low-pass filtering to 3 kHz. For the divalent-blocked cAMP-gated channel, the estimates were $g = 1.07 \pm 0.05$ pS; $p_{max} = 0.51 \pm 0.04$. For the Ca^{2+}-activated Cl^- channel, the estimates were $g = 0.84 \pm 0.12$ pS; $p_{max} = 0.82 \pm 0.04$.

Noise levels during signal amplification

At −50 mV and in the presence of external Ca^{2+}, the ciliary membrane passes a small inward current that is associated with a low level of current noise (Fig. 3 *A*). The addition of cytoplasmic cAMP activates a sequence of two inward ciliary currents (Kleene, 1993b) and increases the current noise (Fig. 3 *B*). An initial steady-state current is carried by Na^+ and Ca^{2+} entering the cilium through the cAMP-gated channels. As internal Ca^{2+} accumulates and gates Cl^- channels, a second steady state is established that includes inward currents through both types of channels (Kleene, 1993b). In the absence of cAMP, the variance and mean current were both low (Fig. 3 *A*). In the presence of cAMP, both mean current and variance were increased (Fig. 3 *B*). As the second phase of cAMP-activated current appeared, there was a further large increase in current, but the current noise did not appear to increase (Fig. 3 *B*).

The results of four such experiments are summarized in Table 3. On average, the combined currents from the basal

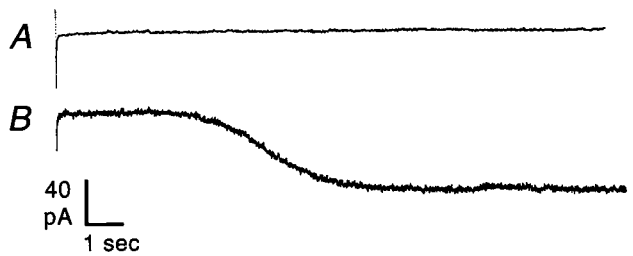

FIGURE 3 Signal-to-noise properties of biphasic ciliary currents activated by cAMP. (*A*) Steady-state current in a cilium in the absence of cytoplasmic cAMP. The potential was jumped from 0 to −50 mV at the start of the record. The mean current was −12 pA, and the current variance was 0.26 pA^2. Note that this current includes both a transmembrane current and current through a shunt at the membrane-pipette seal (Kleene, 1992). In a previous study, the shunt accounted for 65% ± 8% (n = 20) of the input conductance at −50 mV (unpublished data from Kleene, 1992). (*B*) The same cilium was transferred to a cytoplasmic bath containing 100 μM cAMP, and the voltage was again jumped to −50 mV. Two steady-state phases of current resulted, separated by a transition period. For the first phase (0.2–3.5 s), the mean current was −103 pA and the current variance was 1.6 pA^2. For the second phase (8.0–15.0 s), the mean and variance were −170 pA and 1.7 pA^2, respectively. The solutions labeled Biphasic Currents in Table 1 were used for this experiment.

conductance and the first phase of cAMP-activated current totaled −86 pA. The second phase of current contributed an additional −87 pA. Thus the Ca^{2+}-activated Cl^- current allowed a twofold amplification of the primary current through the cAMP-gated channels (Kleene, 1993b; Lowe and Gold, 1993). This amplification was achieved with a minimal increase in current noise. Current variance averaged 1.47 ± 0.33 pA^2 during the first phase of current (including background), and the second phase increased this by just 0.26 ± 0.21 pA^2. The increase in current was significant ($p < 0.01$), whereas the increase in variance was not ($p > 0.3$). In total, the Ca^{2+}-activated Cl^- current accounted for 50% of the total current, but just 13% of the current variance. The variance/mean ratio indicates how much noise accompanies a given increment of receptor current. The combined control and first-phase currents had a variance/mean ratio of −17 ± 2 fA. This was significantly reduced ($p < 0.05$) to −10 ± 1 fA by addition of the second phase of current.

The twofold amplification shown in Fig. 3 and Table 3 was obtained by using a saturating dose of cAMP. Lower levels of cAMP result in a smaller primary current. Reduction of cytoplasmic Ca^{2+} buffering often still allows a maximum secondary Ca^{2+}-activated Cl^- current and thus a larger amplification (Kleene, 1993b). In some cilia, a small basal Ca^{2+} permeability is sufficient to activate a large Cl^- current when Ca^{2+} buffering is reduced (Kleene, 1993b), even though no cAMP is added. In three such cilia, a basal current averaging −8 ± 1 pA was increased to −61 ± 5 pA by addition of the Ca^{2+}-activated Cl^- current. Despite this 7.6-fold increase in current, amplification increased the variance by a factor of only 2.6, from 0.09 ± 0.06 pA^2 to 0.24 ± 0.11 pA^2. Again, the increase in current was significant ($p < 0.02$), but the increase in variance was not ($p > 0.4$).

Frequency dependence of the current noise

The membrane resistance and time constant of olfactory receptor neurons are uncertain. The current records analyzed above were low-pass filtered at 100 Hz, but may still include components that are too fast to be detectable after filtering by the neuronal resistance and capacitance. Fig. 4 shows the frequency dependence of the current records from Fig. 3, *A* and *B*, between 3.4 and 3000 Hz. The relative noise levels among the control and the two phases of the cAMP-activated current summarized in Table 3 were still apparent across most of the frequency spectrum. At most frequencies, little noise was seen in the absence of cAMP (Fig. 4, *open circles*). After the cAMP-gated channels were opened (*open triangles*, corresponding to the first phase of Fig. 3 *B*), there was a substantial increase in noise across the spectrum. Addition of the Ca^{2+}-activated Cl^- current (*open squares*, corresponding to the second phase of Fig. 3 *B*) caused no significant increase in noise at almost any frequency tested. Noise differences between the two phases of the cAMP-activated current were significant at only two frequencies less than 100 Hz (50 Hz and 67 Hz, of 57 frequency bins between 3.4 and 100 Hz, $p < 0.05$).

DISCUSSION

The signal-to-noise properties of the two receptor currents known to mediate olfactory transduction in the frog were measured. The first component of the receptor current is an influx of Na^+ and Ca^{2+} through channels directly gated by cAMP (Nakamura and Gold, 1987). In the absence of divalent cations, this current was associated with the highest noise levels measured in this study. Under physiological conditions, however, the olfactory cilia are bathed in a mucus that contains divalent cations (Joshi et al., 1987; Chiu et al., 1989). External Ca^{2+} and Mg^{2+} caused a great reduction in both the noise and mean current through the cAMP-gated channels (Fig. 2 *A*). Divalent block of cyclic-nucleotide-gated channels has been proposed to increase the signal-to-noise ratio in both visual (Yau and Baylor, 1989) and olfactory (Zufall and Firestein, 1993) transduction.

When sufficient Ca^{2+} enters the cilium through the cAMP-gated channels, a second depolarizing component of the olfactory receptor current appears (Kurahashi and Yau, 1993; Kleene, 1993b; Lowe and Gold, 1993; Firestein and Shepherd, 1995; Zhainazarov and Ache, 1995). This second phase arises from an efflux of Cl^- through ciliary Ca^{2+}-activated Cl^- channels. In isolated cilia, the channels can be activated directly by the addition of cytoplasmic Ca^{2+} (Kleene and Gesteland, 1991b). The resulting ciliary Cl^- current was associated with the lowest current variances measured in this study (Fig. 2). Although the maximum amplitudes of the Cl^- current and the cationic current were

TABLE 3 Signal-to-noise properties of biphasic currents activated by 100 μM cAMP

	Control	First phase	Second phase	Total
Mean current				
pA	−14 ± 1	−72 ± 10	−87 ± 12	−173 ± 17
% total	8 ± 1	42 ± 4	50 ± 4	(100)
Current variance				
pA^2	0.19 ± 0.03	1.28 ± 0.32	0.26 ± 0.21	1.74 ± 0.31
% total	13 ± 3	74 ± 9	13 ± 11	(100)
Variance/mean (fA)	−14 ± 3	−18 ± 3	−3 ± 2	−10 ± 1

For each of four cilia, current was measured in the absence and presence of 100 μM cAMP, as shown in Fig. 3. Holding potential was −40 mV for the first cilium, −50 mV for the second, and −60 mV for the remaining two. For the control record (no cAMP) and for each steady-state phase of the biphasic current in the presence of cAMP, mean current, current variance, and variance/mean were figured. Columns labeled "First phase" and "Second phase" list the additional current and variance added by each phase, not the cumulative values. Correction was made for very slow changes in the mean current, as described in Materials and Methods. The steady-state portions of the biphasic currents were determined by eye and lasted anywhere from 0.65 to 13.5 s. For all but one cilium, the biphasic response was repeated three to six times. Average values were figured for each cilium, and these averages were themselves averaged with equal weighting to give the values shown above.

similar in the presence of divalent cations, the Cl^- current, on average, resulted in less noise.

The noise levels measured can be explained by the properties of the contributing single channels. An expression for the mean macroscopic current I through many channels is

$$I = npi \tag{2}$$

where p is the open probability of a channel, and n and i are as defined for Eq. 1. Substituting Eq. 2 into Eq. 1 shows that the variance σ^2 of a current around its mean is proportional to the square of the unit conductance of the underlying single channels (DeFelice, 1981):

$$\sigma^2 = i^2np(1 - p) \tag{3}$$

In the frog, the cAMP-gated channels have unit conductances of 12–19 pS in the absence of divalent cations (summarized in Frings et al., 1992). However, the effective unit conductance is decreased on the addition of external Ca^{2+} or Mg^{2+} (Zufall and Firestein, 1993; Frings et al., 1995). As expected, external divalent cations decreased both the mean current and the current variance in this study (Fig. 2 *A*). Ca^{2+}-activated Cl^- currents also had very small variances (Fig. 2, Table 2). This is consistent with the underlying channel's very small unit conductance (Larsson et al., 1997; Table 2).

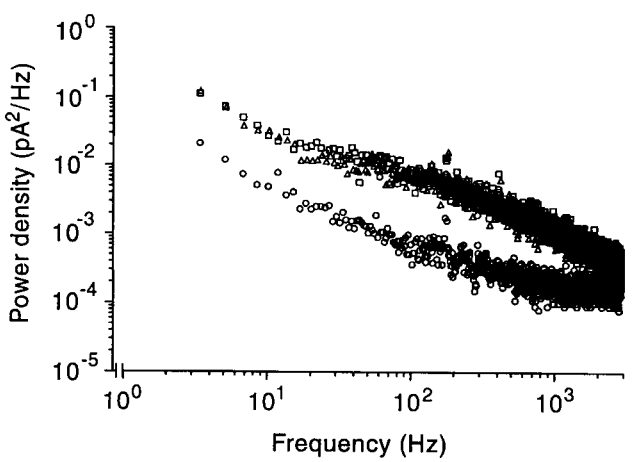

FIGURE 4 Power spectral analysis of the components of the olfactory receptor current. Three power density spectra were calculated from current records such as those shown in Fig. 3. The spectra reflect current in the absence of cAMP (○); current during the first steady-state phase after the addition of cAMP (△); and current during the second phase (□). All recordings were from the same cilium used in Fig. 3.

In the intact olfactory receptor neuron, the secondary Cl^- current serves to amplify the primary cationic current (Kurahashi and Yau, 1993; Lowe and Gold, 1993). In the excised olfactory cilium, it is possible to measure the current noise before and after this amplification. In a single cilium, cAMP activates the two currents in sequence. Two steady-state currents result: the first representing the primary current and the second the sum of both currents (Kleene, 1993b). Amplification by the Cl^- current added very little noise (Fig. 3). Although the cationic and Cl^- currents contributed almost equally to the mean current, the Cl^- current accounted for just 13% of the noise (Table 3).

That this amplification was so optimal reflects in part the experimental design. A saturating level of cAMP was used to generate the biphasic currents (Fig. 3, Table 3), and this is known to also yield a maximum secondary Cl^- current (Kleene, 1993b). Fig. 5 shows the average variance-versus-mean relations for the divalent-blocked cAMP-activated current (*solid curve*) and the Ca^{2+}-activated Cl^- current (*dashed curve*). When the Cl^- current is near saturation (*left end of dashed curve*), a large current is available with little noise. This is because p_{max} for the Cl^- channels is nearly 1.0 (Table 2), at which point the channel noise approaches zero ($\sigma^2 \rightarrow 0$ as $p \rightarrow 1.0$; Eq. 3). The variance of a large cAMP-activated current is high (Fig. 5) because p_{max} for these channels reaches only 0.68 (Table 2). The low p_{max} is consistent with a report that Ca^{2+} stabilizes the closed state of the channel (Zufall et al., 1991). The ratio of the two currents at the threshold of odorant detection is not known.

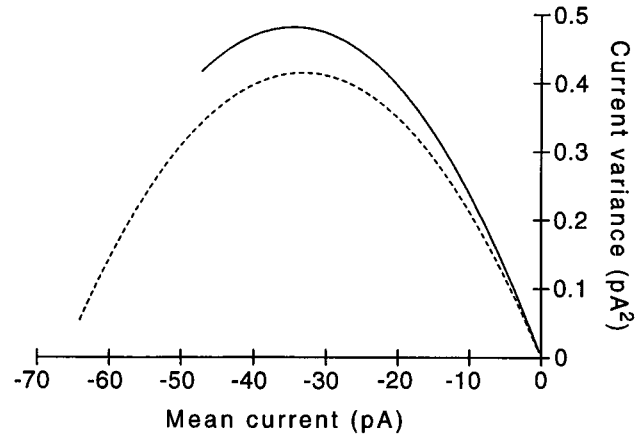

FIGURE 5 Average signal-to-noise properties of the olfactory receptor currents at −50 mV. The mean values of i and n from Table 2 were substituted into Eq. 3 (Discussion) to generate the curves shown. Variance was calculated as p increased from 0 to the mean value of p_{max} shown in Table 2. ——, cAMP-activated current in the presence of external Ca^{2+} and Mg^{2+}. – – –, Ca^{2+}-activated Cl^- current.

At low open probabilities, the two currents have very similar variances (Fig. 5) because of their similar channel densities and unit conductances (Eq. 3, Table 2). For larger currents, though, only the Cl^- current reaches very low noise levels (Fig. 5). In intact olfactory receptor neurons, the Cl^- current is larger than the cationic current at both low and high levels of stimulation (Lowe and Gold, 1993).

In an intact neuron, there is also background noise, even in the absence of stimuli. Knowing whether amplification by the Cl^- current boosts the signal relative to the background noise requires that three questions be answered:

1. Does the Cl^- current selectively amplify the primary receptor current, or are components of the background noise also amplified?

2. Does the amplification process filter (smooth) the primary current before amplifying it?

3. Does the amplification process add substantial noise itself?

The answers to the first two questions are uncertain. To the extent that the background current is not carried by Ca^{2+}, the secondary Cl^- current will selectively amplify the signal (primary current) but not the background. However, it is known that the cilium does have a Ca^{2+} conductance at rest (Kleene, 1993b), perhaps because of spontaneous gating of cyclic-nucleotide-gated channels (Picones and Korenbrot, 1995; Tibbs et al., 1995). Background noise due to this conductance would be amplified along with the cAMP-activated current, and this would confer no signal-to-noise advantage. In an intact neuron, noise in the transduction process itself may cause background fluctuations in the level of cAMP, and this noise could also be amplified (Lowe and Gold, 1995). However, background noise due to K^+ conductances (Kleene, 1992) would not be amplified.

A second question is whether the Cl^- amplification mechanism reduces the noise of the primary signal before amplifying it. This is likely to be the case. Activity of the Cl^- channels does not reflect Ca^{2+} current; it reflects $[Ca^{2+}]_{free}$ in the very restricted ciliary compartment. If removal of Ca^{2+} by diffusion and pumping proceeds much more slowly than Ca^{2+} entry during the odorant response, $[Ca^{2+}]_{free}$ will be proportional to the integral of the Ca^{2+} current over time. Integration or averaging over time would filter out much of the noise present in the primary receptor current before amplifying it. If diffusion and pumping of Ca^{2+} are relatively fast, less of this low-pass filtering would occur. In isolated cilia (Kleene, 1993b) and intact receptor neurons (Kleene and Pun, 1996), accumulation of intraciliary Ca^{2+} is slow enough to noticeably delay the onset of the secondary current. The cost of integration would be a loss of sensitivity to fast, transient changes in the primary receptor current. However, the delay inherent in the second-messenger-mediated transduction process may preclude such transients, even in the primary current. The durations of odorant responses are typically on the order of seconds (e.g., Firestein et al., 1990).

The present study provides an answer to the last of the three questions. Amplification by the Ca^{2+}-activated Cl^- channels contributes little noise. In fact, for saturating currents, the variance from these channels is much smaller than that from the cAMP-gated channels that conduct the primary receptor current. Thus the least noisy receptor current should consist of a small primary current greatly amplified by the secondary current. This has been observed in intact receptor neurons, in which Cl^- carries as much as 85% of the total receptor current (Lowe and Gold, 1993). Having divalent cations in the mucus should optimize the contributions of the two receptor currents in two ways. First, external divalent cations reduce the total primary current (Zufall and Firestein, 1993; Kleene, 1995a; Frings et al., 1995) and its channel noise (Fig. 2). At the same time, the Ca^{2+} current through the cAMP-gated channels increases with external Ca^{2+} (Frings et al., 1995), and it is this Ca^{2+} current that allows amplification by the low-noise Cl^- channels. The result is a total receptor current with the least possible channel noise.

I am grateful to Robert Gesteland, Peter Larsson, Harold Lecar, and King-Wai Yau for helpful comments on the manuscript.

This work was supported by research grant 5 R01 DC 00926 from the National Institute on Deafness and Other Communication Disorders, National Institutes of Health.

REFERENCES

Block, S. M. 1992. Biophysical principles of sensory transduction. *In* Sensory Transduction. D. P. Corey and S. D. Roper, editors. Rockefeller University Press, New York. 1–17.

Boekhoff, I., E. Tareilus, J. Strotmann, and H. Breer. 1990. Rapid activation of alternative second messenger pathways in olfactory cilia from rats by different odorants. *EMBO J.* 9:2453–2458.

Bruch, R. C., and J. H. Teeter. 1990. Cyclic AMP links amino acid chemoreceptors to ion channels in olfactory cilia. *Chem. Senses.* 15: 419–430.

Buck, L., and R. Axel. 1991. A novel multigene family may encode odorant receptors: a molecular basis for odor recognition. *Cell.* 65: 175–187.

Chiu, D., T. Nakamura, and G. H. Gold. 1989. Ionic composition of toad olfactory mucus measured with ion selective microelectrodes. *Chem. Senses.* 13:677–678.

DeFelice, J. L. 1981. Introduction to Membrane Noise. Plenum Press, New York.

Firestein, S., and G. M. Shepherd. 1995. Interaction of anionic and cationic currents leads to a voltage dependence in the odor response of olfactory receptor neurons. *J. Neurophysiol.* 73:562–567.

Firestein, S., G. M. Shepherd, and F. S. Werblin. 1990. Time course of the membrane current underlying sensory transduction in salamander olfactory receptor neurons. *J. Physiol. (Lond.).* 430:135–158.

Frings, S., J. W. Lynch, and B. Lindemann. 1992. Properties of the cyclic nucleotide-gated channels mediating olfactory transduction. *J. Gen. Physiol.* 100:45–67.

Frings, S., R. Seifert, M. Godde, and U. B. Kaupp. 1995. Profoundly different calcium permeation and blockage determine the specific function of distinct cyclic nucleotide-gated channels. *Neuron.* 15:169–179.

Joshi, H., M. L. Getchell, B. Zielinski, and T. V. Getchell. 1987. Spectrophotometric determination of cation concentrations in olfactory mucus. *Neurosci. Lett.* 82:321–326.

Kleene, S. J. 1992. Basal conductance of frog olfactory cilia. *Pflügers Arch.* 421:374–380.

Kleene, S. J. 1993a. The cyclic nucleotide-activated conductance in olfactory cilia: effects of cytoplasmic Mg^{2+} and Ca^{2+}. *J. Membr. Biol.* 131:237–243.

Kleene, S. J. 1993b. Origin of the chloride current in olfactory transduction. *Neuron.* 11:123–132.

Kleene, S. J. 1995a. Block by external calcium and magnesium of the cyclic-nucleotide-activated current in olfactory cilia. *Neuroscience.* 66: 1001–1008.

Kleene, S. J. 1995b. Patch-clamping of whole olfactory cilia. *In* Experimental Cell Biology of Taste and Olfaction/Current Techniques and Protocols. A. I. Spielman and J. G. Brand, editors. CRC Press, Boca Raton, FL. 347–352.

Kleene, S. J., and H. C. Cejtin. 1994. Solving buffering problems with Mathematica software. *Anal. Biochem.* 222:310–314.

Kleene, S. J., and R. C. Gesteland. 1991a. Transmembrane currents in frog olfactory cilia. *J. Membr. Biol.* 120:75–81.

Kleene, S. J., and R. C. Gesteland. 1991b. Calcium-activated chloride conductance in frog olfactory cilia. *J. Neurosci.* 11:3624–3629.

Kleene, S. J., R. C. Gesteland, and S. H. Bryant. 1994. An electrophysiological survey of frog olfactory cilia. *J. Exp. Biol.* 195:307–328.

Kleene, S. J., and R. Y. K. Pun. 1996. Persistence of the olfactory receptor current in a wide variety of extracellular environments. *J. Neurophysiol.* 75:1386–1391.

Kurahashi, T. 1989. Activation by odorants of cation-selective conductance in the olfactory receptor cell isolated from the newt. *J. Physiol. (Lond.).* 419:177–192.

Kurahashi, T., and A. Kaneko. 1993. Gating properties of the cAMP-gated channel in toad olfactory receptor cells. *J. Physiol. (Lond.).* 466: 287–302.

Kurahashi, T., and K.-W. Yau. 1993. Co-existence of cationic and chloride components in odorant-induced current of vertebrate olfactory receptor cells. *Nature.* 363:71–74.

Larsson, H. P., S. J. Kleene, and H. Lecar. 1997. Noise analysis of ion channels in non-space-clamped cables: estimates of channel parameters in isolated olfactory cilia. *Biophys. J.* 72:1193–1203.

Lowe, G., and G. H. Gold. 1991. The spatial distributions of odorant sensitivity and odorant-induced currents in salamander olfactory receptor cells. *J. Physiol. (Lond.).* 442:147–168.

Lowe, G., and G. H. Gold. 1993. Nonlinear amplification by calcium-dependent chloride channels in olfactory receptor cells. *Nature.* 366: 283–286.

Lowe, G., and G. H. Gold. 1995. Olfactory transduction is intrinsically noisy. *Proc. Natl. Acad. Sci. USA.* 92:7864–7868.

Lowe, G., T. Nakamura, and G. H. Gold. 1989. Adenylate cyclase mediates olfactory transduction for a wide variety of odorants. *Proc. Natl. Acad. Sci. USA.* 86:5641–5645.

Nakamura, T., and G. H. Gold. 1987. A cyclic nucleotide-gated conductance in olfactory receptor cilia. *Nature.* 325:442–444.

Pace, U., E. Hanski, Y. Salomon, and D. Lancet. 1985. Odorant-sensitive adenylate cyclase may mediate olfactory reception. *Nature.* 316: 255–258.

Picones, A., and J. I. Korenbrot. 1995. Spontaneous, ligand-independent activity of the cGMP-gated ion channels in cone photoreceptors of fish. *J. Physiol. (Lond.).* 485:699–714.

Shirley, S. G., C. J. Robinson, K. Dickinson, R. Aujla, and G. H. Dodd. 1986. Olfactory adenylate cyclase of the rat. *Biochem. J.* 240:605–607.

Sklar, P. B., R. R. H. Anholt, and S. H. Snyder. 1986. The odorant-sensitive adenylate cyclase of olfactory receptor cells. *J. Biol. Chem.* 261:15538–15543.

Tibbs, G. R., E. H. Goulding, and S. A. Siegelbaum. 1995. Spontaneous opening of cyclic nucleotide-gated channels supports an allosteric model of activation. *Biophys. J.* 68:A253.

Yau, K.-W., and D. A. Baylor. 1989. Cyclic GMP-activated conductance of retinal photoreceptor cells. *Annu. Rev. Neurosci.* 12:289–327.

Zhainazarov, A. B., and B. W. Ache. 1995. Odor-induced currents in *Xenopus* olfactory receptor cells measured with perforated-patch recording. *J. Neurophys.* 74:479–483.

Zufall, F., and S. Firestein. 1993. Divalent cations block the cyclic nucleotide-gated channel of olfactory receptor neurons. *J. Neurophysiol.* 69:1758–1768.

Zufall, F., G. M. Shepherd, and S. Firestein. 1991. Inhibition of the olfactory cyclic nucleotide gated ion channel by intracellular calcium. *Proc. R. Soc. Lond. B.* 246:225–230.